Title

Characterization and Correction of Geometric Distortions in 814 Diffusion Weighted Images.

Journal

PloS one, 11(3)

ISSN

1932-6203

Authors

Treiber, Jeffrey Mark
White, Nathan S
Steed, Tyler Christian
et al.

Publication Date

2016

DOI

10.1371/journal.pone.0152472

Peer reviewed

PLOS | ONE

RESEARCH ARTICLE

Characterization and Correction of Geometric Distortions in 814 Diffusion Weighted Images

Jeffrey Mark Treiber[1,2], Nathan S. White[3], Tyler Christian Steed[1,2,4], Hauke Bartsch[3], Dominic Holland[3], Nikdokht Farid[3,5], Carrie R. McDonald[3,6], Bob S. Carter[2,7], Anders Martin Dale[3☯‡], Clark C. Chen[2,7☯‡*]

1 School of Medicine, University of California San Diego, San Diego, California, United States of America, **2** Center for Theoretical and Applied Neuro-Oncology, University of California San Diego Moores Cancer Center, San Diego, California, United States of America, **3** Multimodal Imaging Laboratory, University of California San Diego, San Diego, California, United States of America, **4** Neurosciences Graduate Program, University of California San Diego, San Diego, California, United States of America, **5** Department of Radiology, University of California San Diego, San Diego, California, United States of America, **6** Department of Psychiatry, University of California San Diego, San Diego, California, United States of America, **7** Department of Neurosurgery, University of California San Diego, San Diego, California, United States of America

☯ These authors contributed equally to this work.
‡ These authors are joint senior authors on this work.
* clarkchen@ucsd.edu

Citation: Treiber JM, White NS, Steed TC, Bartsch H, Holland D, Farid N, et al. (2016) Characterization and Correction of Geometric Distortions in 814 Diffusion Weighted Images. PLoS ONE 11(3): e0152472. doi:10.1371/journal.pone.0152472

Editor: Joseph Najbauer, University of Pécs Medical School, HUNGARY

Received: October 24, 2015

Accepted: March 15, 2016

Published: March 30, 2016

Data Availability Statement: All relevant data are within the paper and its Supporting Information files.

Funding: This work was supported by National Institutes of Health Grants R01 EB00790 and with support by Medtronic. CCC is supported by the Doris Duke Charitable Foundation Clinical Scientist Development Award, the Sontag Foundation Distinguished Scientist Award, the Burroughs Wellcome Fund Career Awards for Medical Scientists, the Kimmel Scholar award, a Discovery Grant from the American Brain Tumor Association, a Grant from Accelerated Brain Cancer Cure, and the William Guy Forbeck Research Foundation. This

Abstract

Introduction

Diffusion Weighted Imaging (DWI), which is based on Echo Planar Imaging (EPI) protocols, is becoming increasingly important for neurosurgical applications. However, its use in this context is limited in part by significant spatial distortion inherent to EPI.

Method

We evaluated an efficient algorithm for EPI distortion correction (EPIC) across 814 DWI scans from 250 brain tumor patients and quantified the magnitude of geometric distortion for whole brain and multiple brain regions.

Results

Evaluation of the algorithm's performance revealed significantly higher mutual information between T1-weighted pre-contrast images and corrected b = 0 images than the uncorrected b = 0 images ($p < 0.001$). The distortion magnitude across all voxels revealed a median EPI distortion effect of 2.1 mm, ranging from 1.2 mm to 5.9 mm, the 5th and 95th percentile, respectively. Regions adjacent to bone-air interfaces, such as the orbitofrontal cortex, temporal poles, and brain stem, were the regions most severely affected by DWI distortion.

material is based upon work supported by the National Science Foundation under Grant No. 1430082. The funders had no role in study design, data collection and analysis, decision to publish, or preparation of the manuscript.

Competing Interests: A.M.D. is a founder and holds equity in CorTechs Labs, Inc., and also serves on its Scientific Advisory Board. A.M.D. is named as an inventor on US Patent US8160319, assigned to the The Regents of the University of California, covering the distortion correction method used in the current report. A.M.D. is a Principal Investigator of a Comprehensive Research Agreement between General Electric Healthcare and the University of California San Diego. The terms of these arrangements have been reviewed and approved by the University of California at San Diego, in accordance with its conflict of interest policies. C.C.C. has grant funding by Medtronic. This does not alter the authors' adherence to PLOS ONE policies on sharing data and materials.

Conclusion

Using EPIC to estimate the degree of distortion in 814 DWI brain tumor images enabled the creation of a topographic atlas of DWI distortion across the brain. The degree of displacement of tumors boundaries in uncorrected images is severe but can be corrected for using EPIC. Our results support the use of distortion correction to ensure accurate and careful application of DWI to neurosurgical practice.

Introduction

Diffusion Weighted Imaging (DWI) is increasingly used to guide the clinical management of neurosurgical brain tumor patients due to the unique ability of this technique to identify regions of high cellularity within tumor and to estimate the integrity of adjacent white matter [1–5]. As a result, three powerful applications of DWI in neurosurgery are target selection for stereotactic biopsy [4], estimation of tumor pathology [6–9], and visualization of fiber tracts during surgical planning [2,3,5]. However, accurate neurosurgical application of DWI is limited by geometric distortion inherent to the imaging modality [10]. Methods for accurate and efficient distortion correction may afford opportunities to maximize the potential of DWI-assisted neurosurgical practice.

The fundamental principle that allows for DWI is the quantification of water diffusion using rapid MR image acquisition [11]. In most clinical applications, this acquisition is achieved through Echo Planar Imaging (EPI), where entire images are acquired in single shots by rapidly reversing the frequency-encoding gradient [12]. While the technique affords high temporal resolution, it has the undesirable effect of introducing significant geometric distortion and intensity variation that result from the interaction between the main magnetic field of the scanner and the patient's anatomy [10,13]. While previous methods have been reported to correct these effects, many are computationally intensive, requiring more time and additional expertise [10,13–21].

We previously reported a method for correcting for such distortions by utilizing an additional non-diffusion weighted (b = 0) DWI volume with reversed phase encoding polarity, requiring only seconds of additional scan time [19]. This additional image possesses equal and opposite distortion magnitude in the plane of acquisition, which can be used to determine regional spatial distortion as the basis for distortion correction. Since its publication, this method has been employed routinely in our clinical and research protocols and thus far has had its clinical utility demonstrated in prostate [22] and breast cancer imaging [23]. Here, we report the application of this method to images from a large cohort of neurosurgical patients with various brain tumors. By mapping the distribution of geometric distortion to a standard brain, our study demonstrates the importance of utilizing distortion correction in neurosurgical applications of DWI.

Methods

Patients

A total of 250 patients with intra-cranial neoplasms at the University of California, San Diego (UCSD) Health Care System were identified retrospectively. The study was approved by the UCSD Institutional Review Board and all participating patients signed informed consent. Imaging was collected beginning in 2010 and at the time of analysis, 822 imaging series were

available. Inclusion in the study required a DWI in addition to artifact free T1-weighted structural images with and without contrast obtained during the imaging session. Eight imaging series were excluded from this study due to excessive imaging artifacts attributable to motion.

Data acquisition

All MR imaging was performed on a 3T Signa Excite HDxt scanner (GE Healthcare, Milwaukee, Wisconsin). As part of the standard protocol we included a 3D volumetric T1-weighted inversion recovery spoiled gradient-echo sequence pre- and post-gadolinium (TE = 2.8 ms, TR = 6.5 ms, TI = 450 ms, flip angle = 8°, FOV = 24 cm; 0.93 x 0.93 x 1.2 mm). Our diffusion protocol consisted of a single-shot pulsed-field gradient Stejskal-Tanner EPI sequence with 4 b-values (b = 0, 500, 1500, and 4000 s/mm^2) and 1, 6, 6, and 15 unique diffusion directions, respectively (TE = 96 ms, TR = 17 s, flip angle = 8°, FOV = 24 cm; 1.875 x 1.875 x 2.5 mm).

Preprocessing

DWI and T1-weighted images were corrected for gradient magnetic field nonlinearity using previously described methods [24]. Diffusion images were additionally corrected for motion and eddy currents [25], and registered to the pre-gadolinium T1-weighted image (T1W) using a rigid-body transform. An inverse transform was applied to resample the T1W to diffusion native space as a basis for evaluation of our algorithm. Additionally, each T1W was registered to a template normal T1W (S1 File) using a rigid-body transform in order to create transforms necessary to place the diffusion data and displacement maps in a common template space. Each registration was manually reviewed to assess accurate alignment.

Distortion correction and quantification

Correction of the patient-specific distortions particular to EPI was performed using the EPI correction algorithm (EPIC) previously described by Holland et al (2010). Briefly, this method utilizes the symmetry of the distortions arising from opposite phase encoding polarities to determine the distortion field that maps voxels back to their true locations (Fig 1A). During acquisition of DWI scans, two non-diffusion-weighted (b = 0) volumes with opposite phase encoding polarities were acquired at the beginning of the scan and used to estimate the voxel-wise distortion field in the anterior-posterior direction (axial plane). The resulting distortion maps were then applied to the remainder of each subjects' diffusion data and transformed to template space.

In order to assess the effectiveness of the algorithm, the Mattes mutual information (MI) similarity metric [26] was used. This histogram-based measure of similarity has been used commonly in neuroimaging to compare images of different modalities [27–29]. This measure was calculated between the T1W in diffusion space and corrected b = 0 and compared to that calculated from the uncorrected posterior-anterior encoded b = 0 scan using a Wilcoxon signed rank test.

To quantify the magnitude of geometric distortion as a function of anatomic location, a cohort-wide displacement atlas was generated by averaging the displacement at each voxel across all registered displacement maps (S2 File).

Results

Algorithm evaluation

Comparisons of the MI similarity metric revealed a higher similarity between T1W and the corrected b = 0 image than the uncorrected b = 0 image in all 814 imaging series ($p < 0.001$,

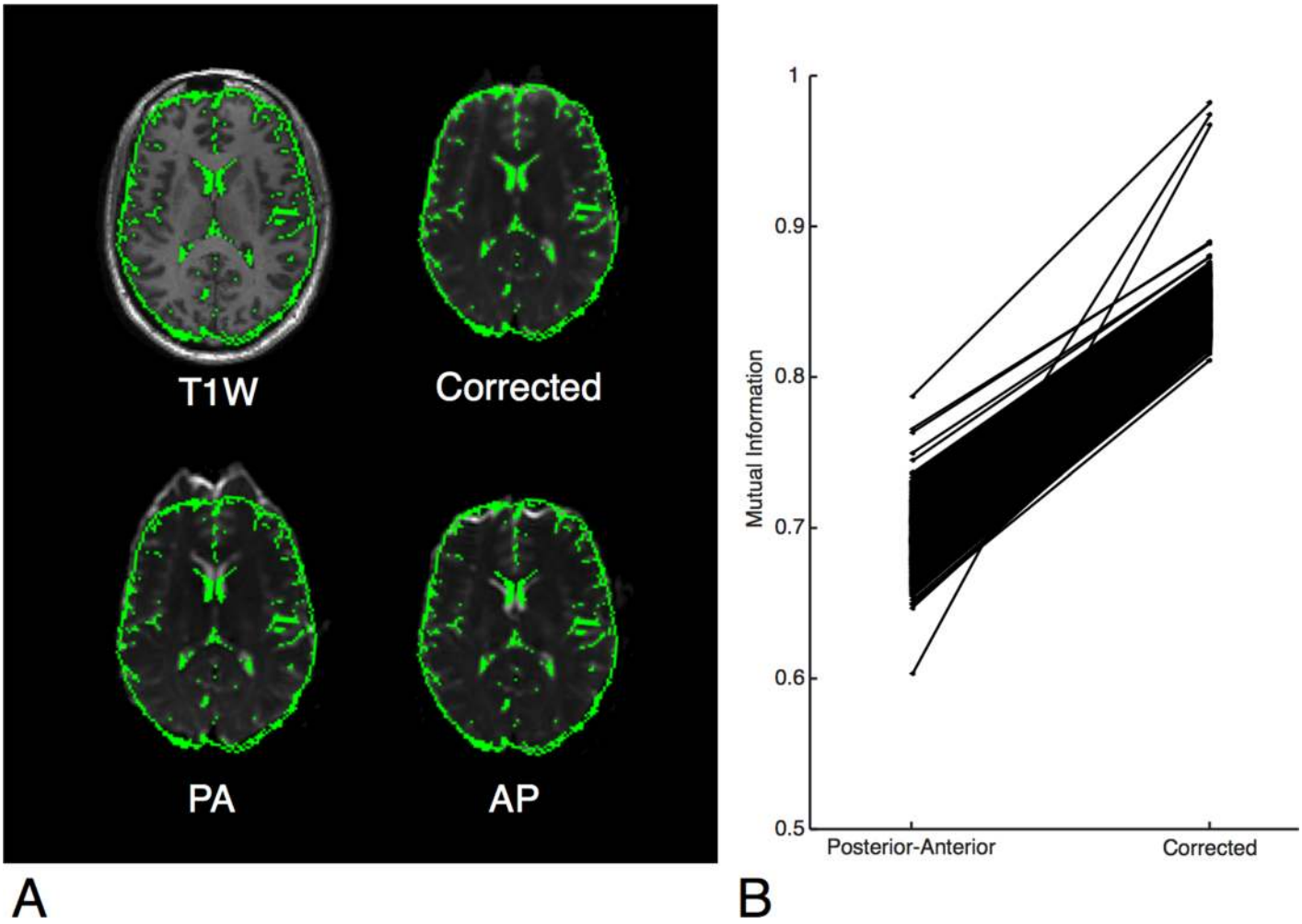

Fig 1. A: Demonstration of the algorithm on a single subject. A mask of the CSF created from the T1W is shown overlaid in green. Top left, subject's T1-weighted MRI image. Top right, subject's corrected b = 0 image. Bottom, subject's uncorrected b = 0 image in both encoding directions is shown, posterior-anterior (PA) and anterior-posterior (AP). The CSF is shown to fit the boundaries of the corrected b = 0 image but not the uncorrected images. This effect is most pronounced in the frontal lobe and anterior aspect of the lateral ventricles. **B:** Mattes mutual information calculated between the T1W and b = 0 images. In all 814 imaging series, the corrected b = 0 image was more similar to the T1W image than the uncorrected b = 0 image.

doi:10.1371/journal.pone.0152472.g001

Fig 1B), indicating that every diffusion image in our cohort was more similar to the T1W after correcting for EPI distortions using EPIC. The displacement atlas displays the average spatial distortion at every voxel (Fig 2). This atlas revealed that the parenchyma adjacent to bone-air interfaces, including the orbitofrontal cortex and temporal pole, had distortions as severe as the brainstem. Quantitative analysis of the displacement atlas showed a median displacement of 2.11 mm, that ranged from 1.2 mm to 5.9 mm, the 5th and 95th percentile, respectively (Fig 3). The regions with the most severe distortions were the brainstem (median distortion d = 5.43 mm), temporal lobe (d = 2.61 mm), and frontal lobe (d = 2.21 mm), while the parietal (d = 1.61 mm) and occipital (d = 1.77 mm) lobes had the least amount of distortion (Fig 3). Within the frontal and temporal lobes, the parenchyma adjacent to the bone-air interfaces, including the orbitofrontal cortex and temporal pole, had distortions as severe as the brainstem (Fig 2). We sought to visualize the impact of DWI related spatial distortion in neurosurgical navigation. To this end, we selected a patient with a tumor with clearly visible boundaries on DWI that extends to tissue adjacent to one of the major bone-air interfaces. To delineate the

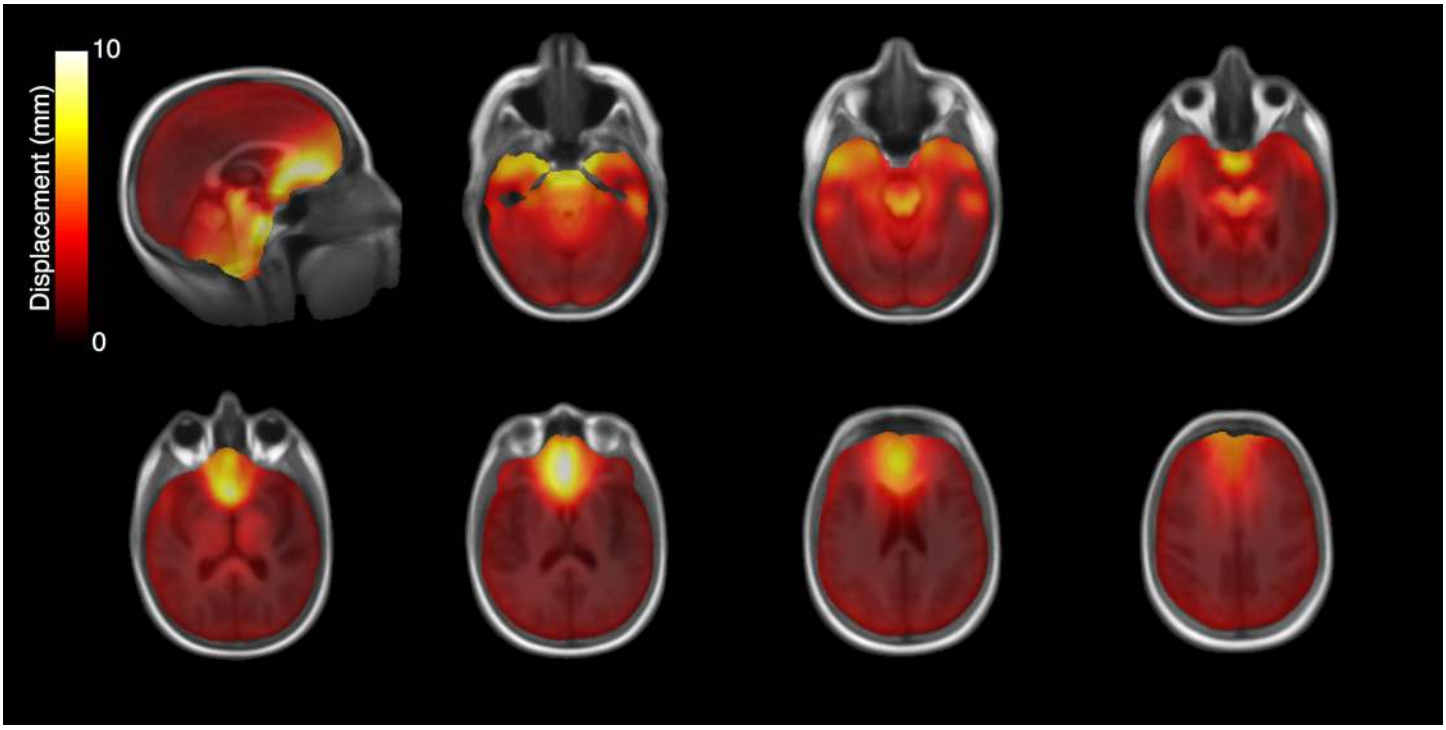

Fig 2. EPI distortion atlas. Average anterior-posterior displacement calculated per voxel over all 814 imaging series registered to a normal brain template.

doi:10.1371/journal.pone.0152472.g002

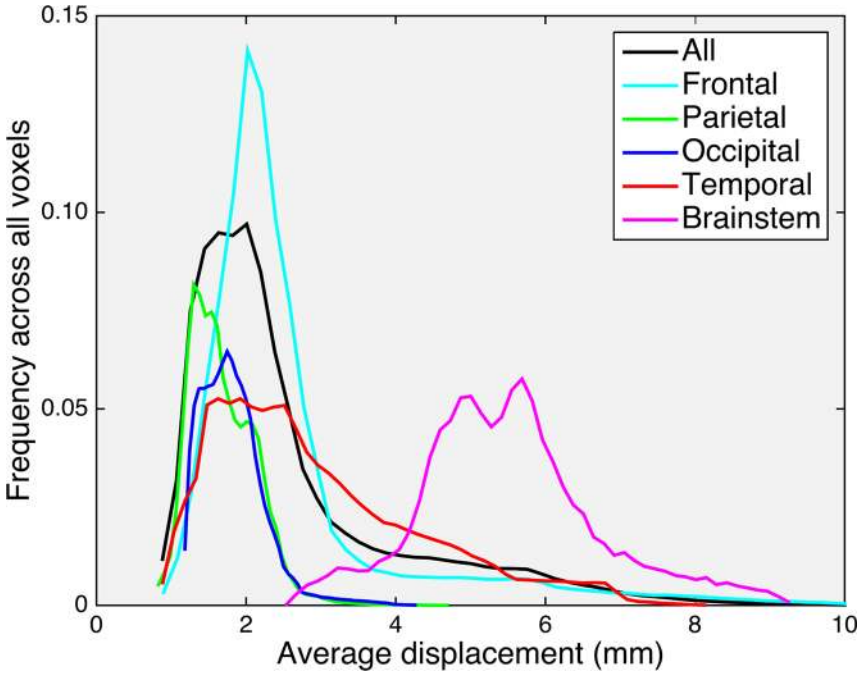

Fig 3. EPI distortion histograms. Anterior-posterior displacement across all voxels within the template brain (black), frontal lobe (cyan), parietal lobe (green), occipital lobe (blue), temporal lobe (red), and brainstem (magenta). Frequency is reported as the fraction of voxels in the region of interest undergoing a given displacement.

doi:10.1371/journal.pone.0152472.g003

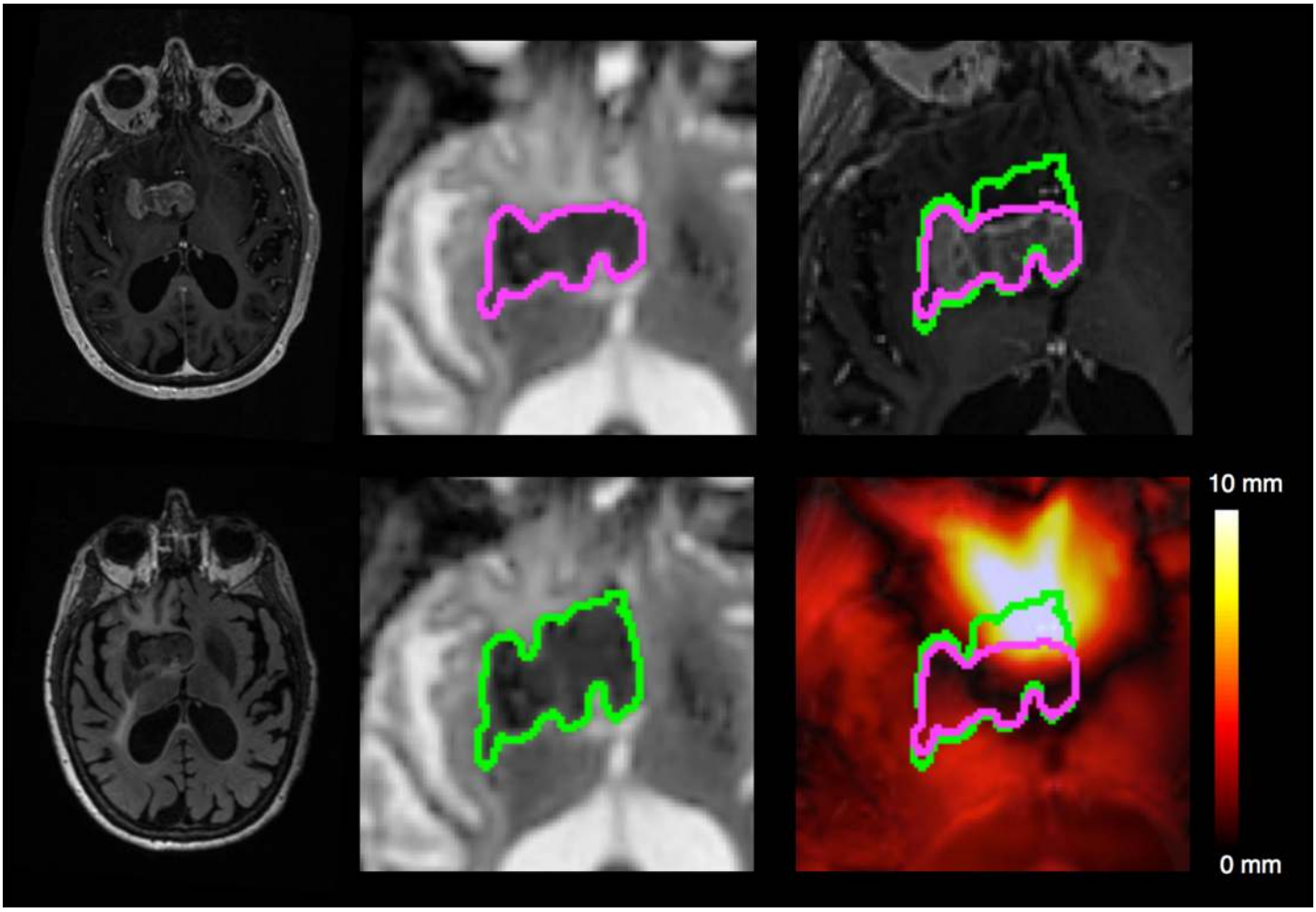

Fig 4. Illustrative example of a tumor's displacement with and without correcting for EPI distortions. Top left, T1-weighted image with contrast. Bottom left, Fluid Attenuated Inversion Recovery image. Middle: ADC calculated from corrected diffusion image (top) and uncorrected diffusion image (bottom) with the regions of diffusion restriction outlined (green/purple). Top right, corrected (purple) and uncorrected diffusion restriction outline (green) overlaid on T1-weighted image with contrast. Bottom right, corrected and uncorrected diffusion restriction outline overlaid on the displacement map.

doi:10.1371/journal.pone.0152472.g004

tumor boundary on diffusion images and assess the effect of image distortion, apparent diffusion coefficient (ADC) maps were generated from the uncorrected and corrected diffusion images using the Stejskal-tanner equation with the diffusion images of the longest diffusion time (b = 4000). As shown in Fig 4, the size of the lesion was artificially increased in the uncorrected ADC image when compared to T1W and Fluid Attenuated Inversion Recovery images while the corrected ADC image more accurately estimated the boundaries of the tumor.

Discussion

Geometric distortion associated with standard DWI sequences has been characterized previously, and poses a significant challenge to achieving high accuracy in DWI-based neurosurgical applications [10,13–19,30]. Here, we assess the significance, applicability, and performance of DWI spatial distortion correction in the context of neurosurgical planning, employing EPIC, a method previously published by our laboratory [19]. We demonstrate that the application of EPIC results in diffusion images considerably closer to the patient's true anatomy as indicated

by T1W. Importantly, the method was integrated into our standard MR clinical protocols, requiring only a single extra image sequence lasting fewer than 5 seconds. The additional short scan time required for EPIC did not adversely impact clinical work-flow and was simple to implement.

Analysis of this large neurosurgical data set of 814 DWIs afforded an opportunity to generate an anatomic atlas of DWI related distortion effects. While DWI distortion affects the entire brain, it is well known [10] (and can be seen from our analysis) that the distortions are most severe in the regions adjacent to bone-air boundaries such as the orbitofrontal cortex, temporal pole, and brain stem. These regions have particular significance for neurosurgeons, as they are common sites for primary brain tumors [31]. We demonstrate that the magnitude of DWI distortion could significantly impact surgical planning and guided stereotactic biopsy by grossly distorting tumor borders as seen in an example subject (Fig 4). These effects may be even more pronounced in other applications of diffusion imaging to neurosurgery such as tractography [32]. The implications of these results together indicate that use of DWI in neurosurgical applications without accurate distortion correction methods like EPIC, may contribute to suboptimal surgical outcomes and ultimately impact the quality of patient care.

There are two potential limitations to our study. First, while 814 DWI images were employed to assess the applicability of distortion correction using EPIC in neurosurgical planning, it is important to note that this study represents a single institutional experience from one scanner. Differences in scanners including hardware, field strength, software version, and shimming can produce significant variation in EPI distortions between institutions. As such, validation of our results by independent institutions is warranted. Second, the integrated sequence used for EPIC is a non-standard prototype used for research that is currently not available commercially. Nevertheless, the sequence requires only an additional scan time of <5 seconds and can be easily integrated into a clinical work flow. While the results reported here are pertinent to DWI sequences, our method can be applied to other EPI based imaging, including perfusion imaging and functional MRI.

Conclusions

DWI is a powerful modality that adds information beyond that afforded by conventional MR imaging. While DWI holds promise to offer benefits to neurosurgical practice, it is currently limited by imaging distortions that result from physical constraints of the image acquisition. Implementation of DWI distortion correction methods like EPIC may help facilitate the development of DWI assisted neurosurgical navigation, and may ultimately improve patient outcomes.

Supporting Information

S1 File. Normal T1-weighted template.
(GZ)

S2 File. EPI distortion atlas. Average anterior-posterior displacement (mm) calculated per voxel over all 814 imaging series registered to a normal brain template (S1 File).
(GZ)

Acknowledgments

This work was supported by National Institutes of Health Grants R01 EB00790 and with support by Medtronic. CCC is supported by the Doris Duke Charitable Foundation Clinical Scientist Development Award, the Sontag Foundation Distinguished Scientist Award, the Burroughs

Wellcome Fund Career Awards for Medical Scientists, the Kimmel Scholar award, a Discovery Grant from the American Brain Tumor Association, a Grant from Accelerated Brain Cancer Cure, and the William Guy Forbeck Research Foundation. This material is based upon work supported by the National Science Foundation under Grant No. 1430082.

Author Contributions

Conceived and designed the experiments: JMT NSW TCS AMD. Performed the experiments: JMT NSW. Analyzed the data: JMT. Contributed reagents/materials/analysis tools: JMT NSW TCS HB DH NF CRM BSC. Wrote the paper: JMT NSW TCS HB DH NF CRM AMD CCC.

References

1. Cho JM, Kim EH, Kim J, Lee S- K, Kim SH, Lee KS, et al. Clinical use of diffusion tensor image-merged functional neuronavigation for brain tumor surgeries: review of preoperative, intraoperative, and postoperative data for 123 cases. Yonsei Med J. 2014; 55: 1303–1309. doi: 10.3349/ymj.2014.55.5.1303 PMID: 25048489
2. Mandelli ML, Berger MS, Bucci M, Berman JI, Amirbekian B, Henry RG. Quantifying accuracy and precision of diffusion MR tractography of the corticospinal tract in brain tumors. J Neurosurg. American Association of Neurological Surgeons; 2014; 121: 349–358. doi: 10.3171/2014.4.JNS131160 PMID: 24905560
3. Potgieser ARE, Wagemakers M, van Hulzen ALJ, de Jong BM, Hoving EW, Groen RJM. The role of diffusion tensor imaging in brain tumor surgery: a review of the literature. Clin Neurol Neurosurg. 2014; 124: 51–58. doi: 10.1016/j.clineuro.2014.06.009 PMID: 25016239
4. Price SJ, Jena R, Burnet NG, Hutchinson PJ, Dean AF, Peña A, et al. Improved delineation of glioma margins and regions of infiltration with the use of diffusion tensor imaging: an image-guided biopsy study. AJNR Am J Neuroradiol. 2006; 27: 1969–1974. PMID: 17032877
5. Zhao Y, Chen X, Wang F, Sun G, Wang Y, Song Z, et al. Integration of diffusion tensor-based arcuate fasciculus fibre navigation and intraoperative MRI into glioma surgery. J Clin Neurosci. 2012; 19: 255–261. doi: 10.1016/j.jocn.2011.03.041 PMID: 22273119
6. Chu HH, Choi SH, Ryoo I, Kim SC, Yeom JA, Shin H, et al. Differentiation of true progression from pseudoprogression in glioblastoma treated with radiation therapy and concomitant temozolomide: comparison study of standard and high-b-value diffusion-weighted imaging. Radiology. Radiological Society of North America; 2013; 269: 831–840. doi: 10.1148/radiol.13122024 PMID: 23771912
7. Lemercier P, Paz Maya S, Patrie JT, Flors L, Leiva-Salinas C. Gradient of apparent diffusion coefficient values in peritumoral edema helps in differentiation of glioblastoma from solitary metastatic lesions. AJR Am J Roentgenol. American Roentgen Ray Society; 2014; 203: 163–169. doi: 10.2214/AJR.13.11186
8. Chen CC, White NS, Farid N, Kobalka P, Hansen L, Pearn M, et al. Pre-operative cellularity mapping and intra-MRI surgery: potential for improving neurosurgical biopsies. Expert Rev Med Devices. 2015; 12: 1–5. doi: 10.1586/17434440.2015.975118 PMID: 25373612
9. White NS, McDonald CR, Farid N, Kuperman JM, Kesari S, Dale AM. Improved conspicuity and delineation of high-grade primary and metastatic brain tumors using "restriction spectrum imaging": quantitative comparison with high B-value DWI and ADC. AJNR Am J Neuroradiol. American Society of Neuroradiology; 2013; 34: 958–64– S1. doi: 10.3174/ajnr.A3327
10. Jezzard P, Balaban RS. Correction for geometric distortion in echo planar images from B0 field variations. Magn Reson Med. 1995; 34: 65–73. PMID: 7674900
11. Turner R, Le Bihan D, Scott Chesnicks A. Echo-planar imaging of diffusion and perfusion. Magn Reson Med. 1991; 19: 247–253. doi: 10.1002/mrm.1910190210 PMID: 1881311
12. Poustchi-Amin M, Mirowitz SA, Brown JJ, McKinstry RC, Li T. Principles and applications of echo-planar imaging: a review for the general radiologist. Radiographics. Radiological Society of North America; 2001; 21: 767–779. doi: 10.1148/radiographics.21.3.g01ma23767
13. Jezzard P. Correction of geometric distortion in fMRI data. Neuroimage. 2012; 62: 648–651. doi: 10.1016/j.neuroimage.2011.09.010 PMID: 21945795
14. Chen NK, Wyrwicz AM. Correction for EPI distortions using multi-echo gradient-echo imaging. Magn Reson Med. 1999; 41: 1206–1213. doi: 10.1002/(SICI)1522-2594(199906)41:6<1206::AID-MRM17>3.0.CO;2-L PMID: 10371453

15. Doran SJ, Charles-Edwards L, Reinsberg SA, Leach MO. A complete distortion correction for MR images: I. Gradient warp correction. Phys Med Biol. IOP Publishing; 2005; 50: 1343–1361. doi: 10.1088/0031-9155/50/7/001 PMID: 15798328

16. Funai AK, Fessler JA, Yeo DTB, Olafsson VT, Noll DC. Regularized Field Map Estimation in MRI. Medical Imaging, IEEE Transactions on. IEEE; 2008; 27: 1484–1494. doi: 10.1109/TMI.2008.923956 PMID: 18815100

17. Gelman N, Silavi A, Anazodo U. A hybrid strategy for correcting geometric distortion in echo-planar images. Magn Reson Imaging. 2014; 32: 590–593. doi: 10.1016/j.mri.2014.02.011 PMID: 24650682

18. Gholipour A, Kehtarnavaz N, Scherrer B, Warfield SK. On the accuracy of unwarping techniques for the correction of susceptibility-induced geometric distortion in magnetic resonance Echo-planar images. Conf Proc IEEE Eng Med Biol Soc. IEEE; 2011; 2011: 6997–7000. doi: 10.1109/IEMBS.2011.6091769 PMID: 22255949

19. Holland D, Kuperman JM, Dale AM. Efficient correction of inhomogeneous static magnetic field-induced distortion in Echo Planar Imaging. Neuroimage. 2010; 50: 175–183. doi: 10.1016/j.neuroimage.2009.11.044 PMID: 19944768

20. Morgan PS, Bowtell RW, McIntyre DJO, Worthington BS. Correction of spatial distortion in EPI due to inhomogeneous static magnetic fields using the reversed gradient method. J Magn Reson Imaging. 2004; 19: 499–507. doi: 10.1002/jmri.20032 PMID: 15065175

21. Andersson JLR, Skare S, Ashburner J. How to correct susceptibility distortions in spin-echo echo-planar images: application to diffusion tensor imaging. Neuroimage. 2003; 20: 870–888. doi: 10.1016/S1053-8119(03)00336-7 PMID: 14568458

22. Rakow-Penner RA, White NS, Margolis DJA, Parsons JK, Schenker-Ahmed N, Kuperman JM, et al. Prostate Diffusion Imaging with Distortion Correction. Magn Reson Imaging. 2015; 33: 1178–1181. doi: 10.1016/j.mri.2015.07.006 PMID: 26220859

23. Teruel JR, Fjøsne HE, Østlie A, Holland D, Dale AM, Bathen TF, et al. Inhomogeneous static magnetic field-induced distortion correction applied to diffusion weighted MRI of the breast at 3T. Magn Reson Med. 2014. doi: 10.1002/mrm.25489

24. Jovicich J, Czanner S, Greve D, Haley E, van der Kouwe A, Gollub R, et al. Reliability in multi-site structural MRI studies: effects of gradient non-linearity correction on phantom and human data. Neuroimage. 2006; 30: 436–443. doi: 10.1016/j.neuroimage.2005.09.046 PMID: 16300968

25. Zhuang J, Hrabe J, Kangarlu A, Xu D, Bansal R, Branch CA, et al. Correction of eddy-current distortions in diffusion tensor images using the known directions and strengths of diffusion gradients. J Magn Reson Imaging. 2006; 24: 1188–1193. doi: 10.1002/jmri.20727 PMID: 17024663

26. Mattes D, Haynor DR, Vesselle H, Lewellyn TK, Eubank W. Nonrigid multimodality image registration. Sonka M, Hanson KM, editors. Medical Imaging 2001. International Society for Optics and Photonics; 2001; 4322: 1609–1620. doi: 10.1117/12.431046

27. Maes F, Vandermeulen D, Suetens P. Comparative evaluation of multiresolution optimization strategies for multimodality image registration by maximization of mutual information. Medical Image Analysis. 1999; 3: 373–386. doi: 10.1016/S1361-8415(99)80030-9 PMID: 10709702

28. Maes F, Collignon A, Vandermeulen D, Marchal G, Suetens P. Multimodality image registration by maximization of mutual information. Medical Imaging, IEEE Transactions on. IEEE; 1997; 16: 187–198. doi: 10.1109/42.563664 PMID: 9101328

29. Chihoub A, Bansal R, Bani-Hashemi A. Performance comparisons of multi-modal medical image registration algorithms. ICIP-02. IEEE; 2002; 3: III–125–III–128 vol.3. doi: 10.1109/ICIP.2002.1038920

30. Hutton C, Bork A, Josephs O, Deichmann R, Ashburner J, Turner R. Image distortion correction in fMRI: A quantitative evaluation. Neuroimage. 2002; 16: 217–240. doi: 10.1006/nimg.2001.1054 PMID: 11969330

31. Ellingson BM, Lai A, Harris RJ, Selfridge JM, Yong WH, Das K, et al. Probabilistic radiographic atlas of glioblastoma phenotypes. AJNR Am J Neuroradiol. American Society of Neuroradiology; 2013; 34: 533–540. doi: 10.3174/ajnr.A3253 PMID: 22997168

32. Irfanoglu MO, Walker L, Sarlls J, Marenco S, Pierpaoli C. Effects of image distortions originating from susceptibility variations and concomitant fields on diffusion MRI tractography results. Neuroimage. 2012; 61: 275–288. doi: 10.1016/j.neuroimage.2012.02.054 PMID: 22401760